Resonance Raman Scattering by Confined LO and TO Phonons in GaAs-AlAs Superlattices

A. K. Sood,[a] J. Menéndez, M. Cardona, and K. Ploog
Max-Planck-Institut für Festkörperforschung, D-7000 Stuttgart 80, Federal Republic of Germany
(Received 5 February 1985)

It is shown that in GaAs-AlAs superlattices the confined longitudinal-optic Raman phonons created via either deformation-potential or Fröhlich electron-phonon interaction are different. This effect is demonstrated by comparison of resonance and off-resonance Raman spectra. Phonons of A_1 symmetry (point group D_{2d}) dominate in resonance, while B_2 phonons are stronger in the off-resonance case. The resonance profile of the A_1 modes is discussed. We also report the observation of confined transverse-optic phonons under extremely resonant conditions.

PACS numbers: 63.20.Dj, 73.40.Lq, 78.30.Gt, 78.40.Fy

The theory of the optical vibrations in thin ionic slabs[1-3] provides insight into the phonon structure of GaAs-AlAs superlattices. For an isolated slab, the z-polarized (z perpendicular to the surface) optical phonons are equivalent to those vibrations in the infinite crystal whose wave vector is given by $m\pi/d$, where d is the thickness of the slab and m an integer.[3] This picture should remain valid for a periodic arrangement of two different ionic slabs, provided that the optical branches of the constituent materials do not overlap. Under these conditions, the vibrations cannot propagate and remain confined in either slab.[4,5] This is the case of GaAs-AlAs superlattices. The series of phonons labeled by m are termed confined phonons and also sometimes inappropriately called "folded" or umklapp phonons.[4,6] Their existence has been demonstrated by investigation of the Raman selection rules[7] and by study of the dependence of the mode frequency on d and m.[4]

In the D_{2d} point group of the superlattice, the z vibrations belong either to the B_2 (m odd) or to the A_1 (m even) representations. Until now only B_2 modes have been clearly identified in Raman scattering.[4] The failure to observe the A_1 phonons has been attributed to the very small value of their diagonal Raman tensor components, as calculated within a polarizability model[4,8]: The corresponding scattering configuration is forbidden in bulk material.

In this paper, we present Raman experiments on GaAs-AlAs superlattices of short period. We discuss here the phonons confined in the GaAs slabs. The off-resonance spectra are dominated by B_2 phonons, as in Ref. 4. However, when the laser energy is near the first electron–heavy-hole exciton, only A_1 modes are detected. We show that this remarkable effect can be traced back to the symmetry properties of the Fröhlich interaction in ionic slabs. We discuss the resonance behavior of the Raman spectrum by confined LO phonons and also show experimental evidence for the confinement of the transverse-optical (TO) branch.

Our measurements were performed at ~ 10 K for three [001]-oriented GaAs-AlAs superlattices grown by molecular-beam epitaxy (MBE). The parameters of the samples are $d_1=20$, $d_2=20$ (sample A); $d_1=20$, $d_2=60$ (B); and $d_1=38$, $d_2=60$ (C), respectively (d_1 and d_2 are the thicknesses of GaAs and AlAs, respectively, in angstroms). Samples A and B consist of 400 periods while sample C has 200 periods. Raman spectra excited with a Coherent Radiation cw dye laser operating with the DCM dye were recorded with a Jarrell-Ash double monochromator in the photon-counting mode. We used the backscattering configuration at the (001) face.

The Raman tensors for A_1 and B_2 phonons with respect to the (x,y,z) crystal axes (z is the superlattice axis) are given by[9]

$$T_{A_1}=\begin{pmatrix} a & 0 & 0 \\ 0 & a & 0 \\ 0 & 0 & b \end{pmatrix}, \quad T_{B_2}=\begin{pmatrix} 0 & d & 0 \\ d & 0 & 0 \\ 0 & 0 & 0 \end{pmatrix}. \tag{1}$$

Hence, we expect to find B_2 phonons in the $z(x,y)\bar{z}$ scattering configuration and A_1 phonons in the $z(x,x)\bar{z}$ configuration. [The symbols within (outside) the brackets indicate the radiation polarization (wave vector).] The selection rule for the B_2 phonons is the same as for dipole-allowed scattering in bulk material. That for the A_1 phonons corresponds to the Fröhlich-interaction–induced (quadrupole-allowed) scattering in the bulk.[10] For bulk GaAs, this "forbidden" scattering is proportional to the square of the scattering wave vector q. It becomes dipole allowed in superlattices because q is replaced by $m\pi/d$.

Figure 1(a) shows typical Raman spectra obtained for the laser frequency ω_L away from all resonances and Fig. 1(b) is for ω_L in resonance with the first electron–heavy-hole exciton of GaAs. The off-resonance spectra are different for the polarized $z(x,x)\bar{z}$ and depolarized $z(x,y)\bar{z}$ configurations, as expected from the selection rules of Eq. (1). The depolarized spectra should correspond to B_2 and the polarized ones to the A_1 modes. The B_2 phonons are characterized by odd m values, and the A_1 phonons by even m values, since their vibrational amplitudes can

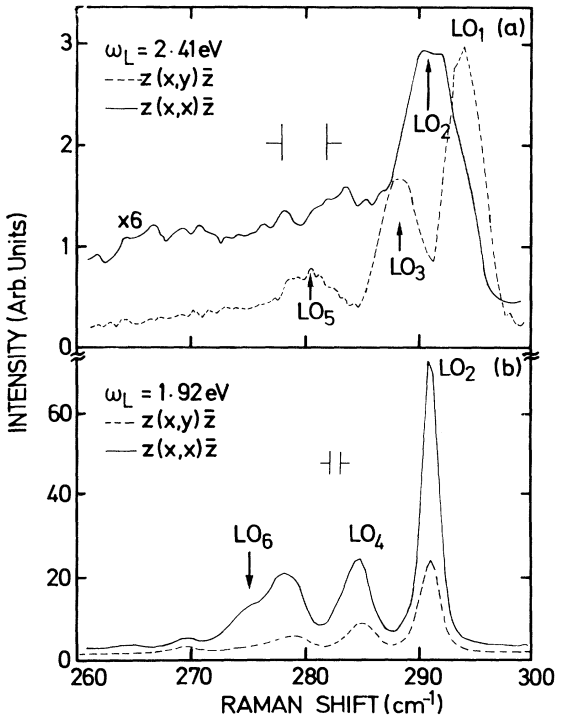

FIG. 1. (a) Off-resonance Raman spectra for polarized and depolarized scattering configurations for sample *B*. (b) Near resonance. The peak on the high-frequency side of LO_6 is believed to be the GaAs-like interface mode (Ref. 11).

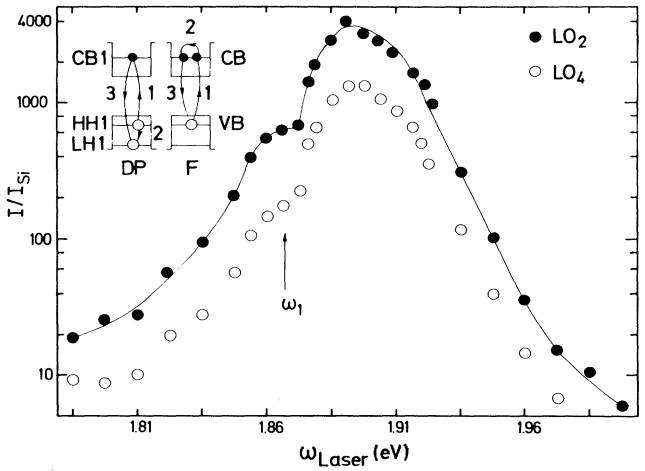

FIG. 2. Observed scattered intensity, measured with respect to that of the Raman phonon of Si, vs incident laser frequency for sample *B*. The inset shows scattering diagrams for deformation-potential (DP) and Fröhlich (F) electron-phonon interaction. The three steps indicated correspond to the three matrix elements in Eq. (3). For the F case a similar diagram with step 2 in the HH1 miniband has to be subtracted. The arrow indicates the calculated energy of the $n = 1$ first heavy-hole exciton frequency. See G. Bastard, Phys. Rev. B **24**, 5693 (1981).

be represented as[3]

$$u_m(B_2) \propto \cos(m\pi z/d_1), \quad m = 1, 3, 5, \ldots,$$
$$u_m(A_1) \propto \sin(m\pi z/d_1), \quad m = 2, 4, 6, \ldots, \tag{2}$$

if the origin of z is taken at the center of the slab. Note that in Ref. 1 the sine and cosine of our Eq. (2) are interchanged. This is due to the fact that the macroscopic electrostatic boundary conditions of Ref. 1 impose a cancellation of the potential at the interface, whereas for the microscopic approach of Refs. 2, 3, and 5 it is rather the ionic displacements (the gradient of the potential) that vanish as a result of the different ionic masses in both slabs.

Near resonance [Fig. 1(b)] the A_1 modes become dominant for both polarizations. Their resonance is shown in Fig. 2. It has an asymmetric profile with a peak for the scattered frequency ω_S equal to the exciton frequency ω_1 (outgoing channel) and a shoulder for $\omega_L = \omega_1$ (incoming channel). Although the incoming channel is not as well resolved as in previous experiments,[12] as a result of the broadening inherent to very thin layers, our interpretation of the resonant profile is supported by the excellent agreement between the observed and calculated value of ω_1 (Fig. 2), for which we use an independent x-ray determination of the layer thicknesses, and by the fact that the outgoing resonance (the maximum of Fig. 2) has an anti-Stokes shift of one phonon energy. Moreover, the maximum of the resonance of the second-order Raman spectrum by confined phonons is about two phonon energies higher than ω_1, in perfect agreement with the expected stronger outgoing resonance for fourth-order processes.[13]

The dominance of the A_1 modes near resonance can be explained by an analysis of how these phonons couple to the electronic system. As a result of the spatial confinement, the conduction band (CB), and the heavy- (HH) and light-hole (LH) valence bands in the superlattice split into a series of minibands (CB1, CB2, etc.).[14] Some of these levels are indicated in the inset of Fig. 2. Not shown is the **k** dependence of the minibands.

The Raman efficiency can be written[9]

$$|\hat{\boldsymbol{\epsilon}}_S \cdot \mathbf{R} \cdot \hat{\boldsymbol{\epsilon}}_L|^2 \propto \left| \sum_{ij} \frac{\langle 0|\hat{\boldsymbol{\epsilon}}_S \cdot \mathbf{p}|i\rangle \langle i|H_{eL}|j\rangle \langle j|\hat{\boldsymbol{\epsilon}}_L \cdot \mathbf{p}|0\rangle}{(\omega_L - \omega_j)(\omega_S - \omega_i)} \right|^2, \tag{3}$$

where **p** is the momentum operator and H_{eL} the electron-phonon interaction. The intermediate states $|i\rangle$, $|j\rangle$ are the excitons formed with an electron in the CB minibands and a hole in the HH or LH minibands. The Hamiltonian H_{eL} is $H_{eL} = H_{DP} + H_F$, where H_{DP} is the (short-range) deformation-potential interaction and H_F the Fröhlich

interaction associated with the macroscopic electric field of the LO phonons. The operator H_{DP} produces the Raman tensor for B_2 phonons in Eq. (1).

Because H_{DP} only couples the LH and HH valence bands, the states $|i\rangle$, $|j\rangle$ in Eq. (3) cannot be the same, and the two denominators do not resonate simultaneously. The Fröhlich interaction, on the other hand, has intraband matrix elements, i.e., the strongly resonant situation $|i\rangle = |j\rangle$ becomes possible in Eq. (3). In our case, the photon energy ω_L is swept near the exciton $|\omega_1\rangle$, formed with the CB1 and HH1 minibands, thus fixing the index i. Although in principle H_F can couple different conduction (or valence) minibands, for $\omega_L \sim \omega_1$ we can restrict $|j\rangle$ to $|\omega_1\rangle$: Only this term leads to two nearly resonant denominators in Eq. (3). Because the phonon amplitudes are proportional to the polarization, which in turn is proportional to the gradient of the Fröhlich potential, we obtain from Eq. (2)

$$\langle \mathrm{CB1}|H_F|\mathrm{CB1}\rangle \propto \int_{-d_1/2}^{d_1/2} dz \cos^2(\beta z) \times \begin{cases} \sin(m\pi z/d_1), & m = 1,3,5,\ldots, \\ \cos(m\pi z/d_1), & m = 2,4,6,\ldots, \end{cases}$$

since $|\mathrm{CB1}\rangle \propto \cos(\beta z)$, where $\beta^2 = 2mE/\hbar^2$ and E is the energy of the $|\mathrm{CB1}\rangle$ level.[14] The same result holds for the $|\mathrm{HH1}\rangle$ level. Thus the Fröhlich coupling *cancels* for B_2 phonons. This explains why only A_1 phonons are seen in resonance. Excitonic effects should not alter substantially this symmetry argument. The conclusions here are exactly reversed for longitudinal-acoustic phonons, since the polarization they produce is proportional to the strain (piezoelectric interaction) and not to the displacement.[15]

The standard Fröhlich mechanism implies polarized scattering, while our results indicate that the Fröhlich-induced A_1 phonons are seen near resonance both in the $z(x,x)\bar{z}$ and the $z(x,y)\bar{z}$ configurations. Furthermore, they are also present in the $z(x \pm y, x \pm y)\bar{z}$ configurations. Thus, an additional scattering mechanism is needed to explain the presence of depolarized scattering. Such mechanism may be impurity-induced Fröhlich-interaction scattering,[16] which is known to be rather important in bulk GaAs.[13] In this case, Eq. (3) has to be modified to include an additional matrix element for exciton-impurity scattering and an additional energy denominator.[13] Impurity-induced Raman scattering would also naturally explain the stronger outgoing resonance in Fig. 2. Such behavior is expected because of double-resonance effects.[13] We may point out that impurities, like carbon incorporated during MBE growth, are important for stabilizing the AlAs layers in GaAs-AlAs superlattices.[17] An alternative explanation for the stronger outgoing resonance, based on scattering between different minibands,[12] fails to explain our experimental asymmetry in the resonance profile. The fact that depolarized Raman scattering by LO phonons in bulk GaAs[18] is weaker than in superlattices might be related to the different k-space integrations in the calculation of the Raman tensor for both cases.

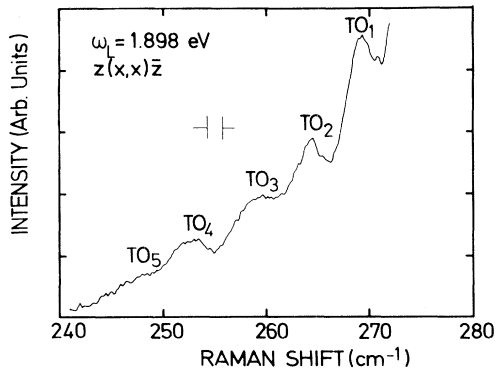

FIG. 3. Resonant Raman spectra in polarized configuration in the GaAs TO region for sample B.

Figure 3 shows spectra obtained in the region near and below the TO frequency of GaAs. The series of peaks displayed in this figure is only observed for ω_S very close to ω_1. We thus assume that we are seeing confined TO phonons which, although symmetry forbidden, become allowed under extreme resonance. Forbidden TO Raman scattering has also been observed in doped GaAs.[19] The confined phonons are labeled by an index m which is equivalent to that of Eq. (2). Note that both odd- and even-m TO phonons are observed, while for LO phonons only even m's are seen near resonance.

Keeping in mind the correspondence between the confined-phonon and the slab-mode frequencies, we plot in Fig. 4 the theoretical dispersion relations for LO and TO phonons in bulk GaAs[20] together with the confined-phonon frequencies vs $q = m\pi/d_1$. We notice that the TO phonons map extremely well onto the dispersion relation of the bulk, thus confirming our assignment. This mapping is not as good for the confined LO phonons, which clearly fall higher than the bulk theoretical curve. We note, however, that our result agrees better with neutron scattering data[21] for $q \leq 0.7 \times 2\pi/a_0$ (a_0 is the lattice constant). Unfortunately, the accuracy of the mapping cannot be satisfactorily checked, because of the large error bars of the only neutron data available.[21] The deviations of the confined LO frequencies from the theoretical predictions still remain present in a recent calculation of the phonon structure of superlattices.[5]

We thank H. Hirt, P. Wurster, and A. Fischer for

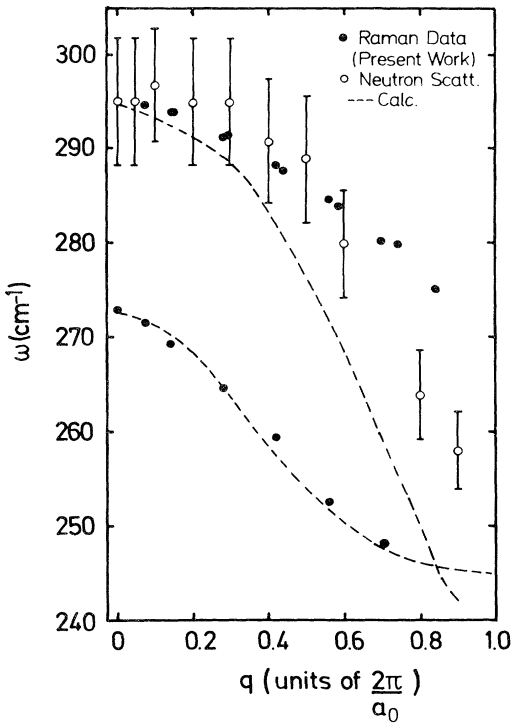

FIG. 4. Observed LO_m and TO_m (all samples) frequencies vs $m\pi/d_1$. Also shown are the neutron scattering data (Ref. 21) displaced by 10 cm^{-1} to account for temperature shift and to match our $q=0$ phonon frequency. Dotted curves are the calculated dispersion curves for the bulk, based on the adiabatic bond-charge model (Ref. 20). The theoretical curve for the TO branch has been shifted up to match the TO Raman frequency in bulk GaAs.

technical assistance and G. Kanellis for discussions.

---

[a]On leave from Materials Science Laboratory, Reactor Research Center, Kalpakkam-603102, India.

[1]R. Fuchs and K. L. Kliewer, Phys. Rev. **140**, A2076 (1975).

[2]W. E. Jones and R. Fuchs, Phys. Rev. B **4**, 3581 (1971).

[3]G. Kanellis, J. F. Morhange, and M. Balkanski, Phys. Rev. B **28**, 3406 (1983).

[4]B. Jusserand, D. Paquet, and A. Regreny, Phys. Rev. B **30**, 6245 (1984). The confined phonons are called "folded" phonons in this paper where, in fact, it is shown that the folding or umklapp representation is not appropriate for optical phonons of GaAs-AlAs superlattices because of the large difference in the corresponding dispersion relations. The approximate frequencies of the confined phonons can be obtained from the bulk dispersion relations $\omega_{1,2}(q)$ by insertion of $q=m\pi/d_{1,2}$ ($d_{1,2}$ are the thicknesses of the two constituent slabs) rather than $q=2m\pi/(d_1+d_2)$, as expected for folding.

[5]S. K. Yip and Y. C. Chang, Phys. Rev. B **30**, 7037 (1984).

[6]G. Sai-Halasz, A. Pinczuk, P. Y. Yu, and L. Esaki, Solid State Commun. **25**, 381 (1978). Apart from the inappropriate assignment of their peaks to "umklapp" processes (see comment of Ref. 4), the interpretation of the experimental data of Sai-Halasz *et al.* in terms of confined phonons has some drawbacks, as pointed out by R. Merlin *et al.*, Appl. Phys. Lett. **36**, 43 (1980). We rather believe these peaks to be interface modes [see A. K. Sood *et al.*, following Letter [Phys. Rev. Lett. **54**, 2115 (1985)]].

[7]J. E. Zucker, A. Pinczuk, D. S. Chemla, A. Gossard, and W. Wiegmann, Phys. Rev. Lett. **53**, 1280 (1984).

[8]A. S. Barker, Jr., J. L. Merz, and A. C. Gossard, Phys. Rev. B **17**, 3181 (1978).

[9]W. Hayes and R. Loudon, *Scattering of Light by Crystals* (Wiley, New York, 1978).

[10]M. Cardona, in *Light Scattering in Solids II,* edited by M. Cardona and G. Güntherodt, Topics in Applied Physics, Vol. 50 (Springer-Verlag, Berlin, 1982), p. 19.

[11]Sood *et al.*, Ref. 6.

[12]J. E. Zucker, A. Pinczuk, D. S. Chemla, A. Gossard, and W. Wiegmann, Phys. Rev. Lett. **51**, 1293 (1983).

[13]J. Menéndez and M. Cardona, Phys. Rev. B **31**, 3696 (1985).

[14]For a review, see D. S. Chemla, Helv. Phys. Acta **56**, 607 (1983).

[15]C. Colvard, R. Merlin, M. V. Klein, and A. C. Gossard, Phys. Rev. Lett. **45**, 298 (1980); C. Colvard *et al.*, Phys. Rev. B **31**, 2080 (1985).

[16]A. A. Gogolin and E. I. Rashba, Solid State Commun. **19**, 1177 (1976).

[17]J. C. Phillips, J. Vac. Sci. Technol. **19**, 545 (1981).

[18]J. Menéndez, A. K. Sood, and M. Cardona, unpublished.

[19]D. Olego and M. Cardona, Phys. Rev. B **24**, 1217 (1981).

[20]K. C. Rustagi and W. Weber, Solid State Commun. **18**, 673 (1976).

[21]G. Dolling and J. L. T. Waugh, in *Lattice Dynamics,* edited by R. F. Wallis (Pergamon, London, 1965), p. 19.